Two-Dimensionalization of Electron Gas in *n*-InSe Crystals Induced by Electron Irradiation

I.V. Mintyanskii, P.I. Savitskii* and Z.D. Kovalyuk

I.M. Frantsevich Institute for Problems of Materials Science of the National Academy of Sciences of Ukraine, Chernivtsi Branch, Iryna Vilde Str. 5, Chernivtsi 58001, Ukraine

(Received July 2, 2019; revised version July 22, 2019; in final form December 16, 2019)

The effect of a high-energy (9.2 MeV) electron irradiation with a dose of $10^{14}e$ cm^{-2} on the transport of charge carriers across the layers and the conductivity anisotropy is investigated in the range 80 to 400 K for layered *n*-InSe crystals. It is established that the anisotropy ratio $\sigma_{\perp C}/\sigma_{\parallel C}$, being initially high and slightly dependent on temperature, abruptly increases after the *e*-irradiation and varies with temperature according to an exponential law. The obtained results are explained within a model, which along with 3D electrons predicts the presence of 2D carriers contributing only to charge transport along the layers. It is shown that the role of the latter becomes stronger after the *e*-irradiation.

DOI: 10.12693/APhysPolA.137.1031

PACS/topics: indium selenide, electron irradiation, 2D-3D model, conductivity anisotropy

1. Introduction

Because of sensitivity to wide spectrum of electromagnetic radiation, layered III–VI compounds in their bulk and film forms are promising materials for photoelectronics. Mechanical coupling of their nanodimensionally thick samples with other layered materials, especially high-conductivity transparent graphene [1, 2], as well as controlled oxidation [3] gave opportunities to create effective 2D optoelectronic devices based on quantum confinement effects [4]. For such applications *n*-InSe seems to be the most promising because it stands out, as compared to other layered 2D chalcogenides, for the highest mobility of charge carriers along the layers, i.e., $\approx 10^3$ cm^2/(V s) at room temperature (RT). Its resistance to various types of radiation exposure, higher in comparison to conventional semiconductors, extends area of applications.

Layered crystalline structure of materials causes some peculiarities, in particular the existence of planar defects between separate layers. As an example one can consider defects of the form of $Zn_2In_2S_5$ layers guested in the layered $ZnIn_2S_4$ crystals. These defects determine high values of the conductivity anisotropy $\sigma_{\perp C}/\sigma_{\parallel C} = 10^3 \div 10^4$ (the ratio of the conductivity along the layers $\sigma_{\perp C}$ to that across to them $\sigma_{\parallel C}$), which was thought to be due to tunneling through thin and high barriers [5, 6].

In layered III–VI crystals the closed chemical bonds within a separate layer (four monoatomic planes in the sequence Se–In–In–Se in the case of InSe) and a wide enough spacing ($\approx$ 3.2 Å) between the layers, coupled together by weak van der Waals (vdW) forces, promote planar defects of another type. In real InSe crystals are stacking faults between different polytypes — the prevailing γ- and minor ε-modifications.

*corresponding author; e-mail: petersa@i.ua

Depending on crystals' perfection, the values of conductivity anisotropy can vary from several units for the most perfect samples, when the anisotropy ratio is nearly independent of temperature, to values of $10^4 \div 10^5$ obeying the relation $\sigma_{\perp C}/\sigma_{\parallel C} \sim \exp(\Delta E_b/k_B T)$ at low temperatures T. Here ΔE_b is the energy barrier related to interlayer disordering and k_B is the Boltzmann constant. Staying within the concept of exclusively free electron conductivity in *n*-InSe crystals, high values of anisotropy ratio were explained in the literature assuming that the three-dimensional (3D) electrons exist in the conduction band and two-dimensional (2D) carriers contribute only to conductivity along the layers. At first, electrical characteristics were explained assuming the existence of 2D electric sub-bands situated in the range of interlayer planar aggregates of donor impurities [7–10]. Later, many experimental data have been analyzed within a model predicting the existence of 2D subbands located in the vicinity of the stacking faults separating thin ($\approx$ 100 Å) ranges of ε-InSe from the dominant γ-polytype [11–14]. As for the conductivity anisotropy data in *n*-InSe [8, 13–16], because of many unknown parameters their analysis was complicated, only the energy barrier ΔE_b was estimated and there are no data about the densities of 3D and 2D electrons and effects on them of high-energy irradiations.

However, the above mentioned experimental data do not contain direct indications on the existence of two types of carriers in *n*-InSe (extrema in temperature dependences of the Hall coefficient R_H and the Hall mobility along the layers $\mu_{\perp C}$). We observed such peculiarities first in electrical properties of *n*-InSe after high-energy electron irradiation (9.2 MeV) of pristine samples with a concentration of charge carriers $n \approx 1.5 \times 10^{14}$ cm^{-3} at 80 K [17]. It enabled to carry out rigorous numerical modeling within a 3D–2D approach.

Here, we first represent investigations of the influence of the same electron irradiation fluence ($10^{14}e$ cm^{-2})

on conductivity across the layers $\sigma_{\parallel C}$ and anisotropy $\sigma_{\perp C}/\sigma_{\parallel C}$ for n-InSe samples from the same intentionally undoped ingot as in [17]. The obtained results are analyzed within a model containing two types of carriers and the contributions of tunnel and activation mechanisms to charge transport across the layers are estimated and the energy barrier and the densities of 3D and 2D electrons are determined as well. To our knowledge, it is the first numerical analysis for the $\sigma_{\parallel C}$ conductivity in n-InSe crystals based on this model.

2. Experimental

Samples for investigations were prepared from a single crystal ingot of undoped n-InSe grown by the Bridgman method from a non-stoichiometric melt $In_{1.03}Se_{0.97}$. Before our experiments the ingot was kept at RT for 10 years. The irradiation of the samples with accelerated electrons (E = 9.2 MeV) has been carried out at room temperature by means of an electron accelerator, KUT-10. The beam of electrons at the tantalum foil was developed in a way to have the area with uniformly distributed density of electrons equal to 400×50 mm^2. The samples under investigations were irradiated with a dose of 30 kGy. Taking into account that the degree of deceleration of penetrating electrons is about 10 MeV cm^{-1}, energy losses for our samples did not exceed 10%. Therefore, one can suppose that the generation of radiation damage occurs nearly uniformly on the whole bulk of the samples.

Mechanical properties of layered InSe crystals do not allow to cut samples with dominant dimension along the C axis. That is why for measurements of the $\sigma_{\parallel C}$ conductivity we used a four-contact method with the indium contacts located on the opposite cleaved surfaces (inset in Fig. 1). In our experiments the spacing between the current and probe voltages on each cleaved surface did not exceed 0.3 mm. The current contacts covered almost the whole surface on each side (∼80%) and a probe voltage was measured between a pair of close to them small area contacts. Samples' dimensions were typically 5×3 mm^2 (cleaved surface) and 0.6 mm thick. This method was proposed in [18] where it was shown that because of the high anisotropy of the material, voltage between the small probe contacts was very close to the potential difference between the current ones. Later this technique was used for measurements of "vertical" conductivity in n-InSe [8, 13–15].

We carried out our measurements in the range 80 K to 300 K (pristine samples) and to 400 K (after irradiation). The restriction in T to 300 K for the pristine samples was used to avoid possible dissociation of interlayer impurity aggregates.

Temperature dependences of the conductivity along the layers $\sigma_{\perp C}$ and the Hall coefficient R_H were measured, as well. These d.c. measurements were carried out with a constant magnetic field of 0.75 T along the C axis for samples in the form of a rectangular parallelepiped with

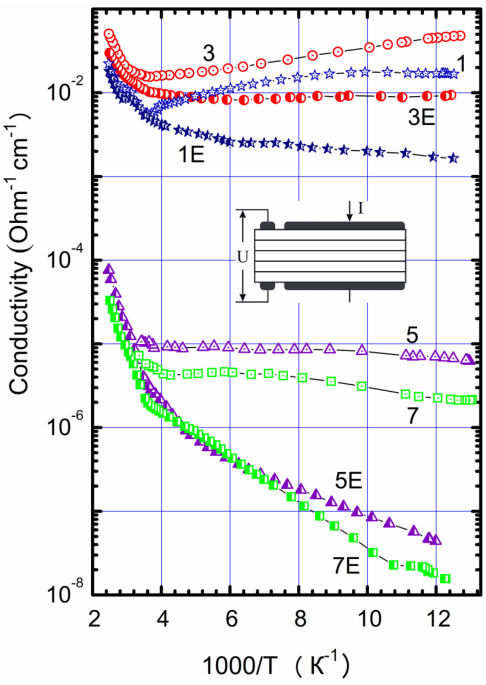

Fig. 1. Temperature dependences of the conductivity along (1, 1E, 3, and 3E) and across the layers (5, 5E, 7, and 7E) for initial (1, 3, 5, and 7) and e-irradiated (1E, 3E, 5E, and 7E) samples of n-InSe. Inset — scheme of $\sigma_{\parallel C}$ measurements.

typical dimensions $10 \times 2.5 \times 0.8$ mm^3. High-purity In contacts to them were soldered in the conventional six-probe configuration. To delete possible effect of residual photoconductivity, the samples were kept in dark for 3 days before measurements.

Samples 3, 5, and 7 were prepared from the same disk-like part of a single crystal n-InSe ingot. After measurements of the temperature dependences of electrical characteristics ($\sigma_{\perp C}(T)$ and $R_H(T)$ for sample 3 and $\sigma_{\parallel C}(T)$ for samples 5 and 7) they were simultaneously irradiated and then measured again. From the ratio of the conductivity components $\sigma_{\perp C}$ and $\sigma_{\parallel C}$ for two pairs of samples (3 and 5) as well (3 and 7) the conductivity anisotropy was determined before and after irradiation. Regarding sample 1, for which electrical parameters along the layered were measured, it was prepared from another n-InSe ingot and irradiated separately. Note that all the measurements of the electrical characteristics before and after electron irradiation were carried out for the same samples keeping the same contacts.

3. Results and discussion

Temperature dependences of the conductivities along and across the layers as well as those for their anisotropy $\sigma_{\perp C}/\sigma_{\parallel C}$ for the initial and irradiated InSe samples are shown in Figs. 1 and 2, respectively, and numerical values of the parameters are listed in Table I. Both before and

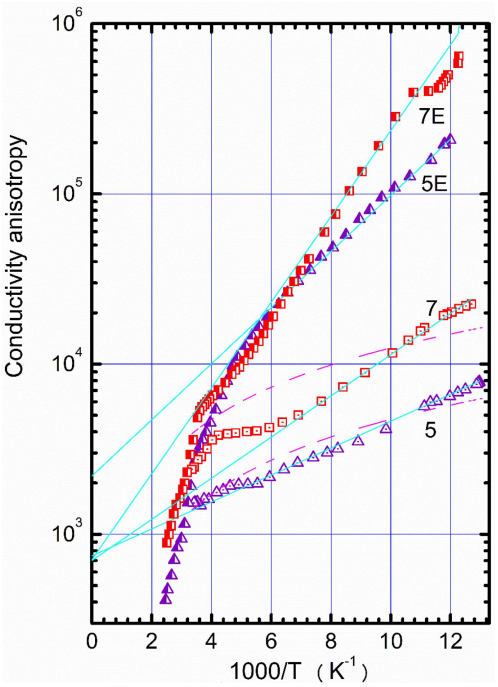

Fig. 2. Temperature dependences of the conductivity anisotropy for initial (5 and 7) and *e*-irradiated (5E and 7E) samples of *n*-InSe. Symbols — experimental data. Lines — calculated dependences for the activation (solid) and tunnel (dash) models.

after the irradiation, the transverse conductivity is much lower than the longitudinal one for both the samples. Note that for pristine samples 5 and 7 at $T < 300$ K there is only an insignificant increase of $\sigma_{\parallel C}$ with temperature. As a result, at low temperatures we have an evident conductivity anisotropy, which at 80 K achieves and even exceeds a value of 10^4. It slightly decreases with increasing temperature to 300 K — less than by an order of magnitude. The electron irradiation leads to both a significant decrease of the conductivity $\sigma_{\parallel C}$ (more than by a factor of 10^2) and its activation increase with temperature. After the *e*-influence the ratio $\sigma_{\perp C}/\sigma_{\parallel C}$ considerably increases at 80 K (to 2.5×10^5 and 7.0×10^5 for samples 5E and 7E, respectively) and exponentially decreases with increasing T. The found increase of $\sigma_{\perp C}/\sigma_{\parallel C}$ is preferably due to the decrease of $\sigma_{\parallel C}$. Note that such high values of the anisotropy ratio in undoped *n*-InSe have not been observed earlier.

Figure 3 shows temperature dependences of the Hall coefficient R_H and the Hall mobility along the layers $\mu_{\perp C}$ for pristine and irradiated sample 1. They reproduce the data very well for sample 3 in [17] and are presented here mainly as an evident reason for the application of a 2D-3D model below. In the range $T < 250$ K the variation of the Hall coefficient with temperature is caused by a shallow donor level (18.5 meV) [13] typical for undoped *n*-InSe. In this range the decrease of $\mu_{\perp C}$ with increasing T is caused by the dominant interaction of free electrons with homopolar optical phonons polarized along the C axis [19]. Such dependences of R_H and $\mu_{\perp C}$ result in a "metallic" behavior of the $\sigma_{\perp C}(T)$ conductivity. At $T > 300$ K the concentration of electrons abruptly increases due to their activation from a deep donor (0.49 eV) [17]. As for irradiated sample 1E, the existence of the maximum in the $R_H(T)$ dependence and a non-monotonous variation of $\mu_{\perp C}$ with T are its distinguished peculiarities. Above 160 K the Hall coefficient starts to increase and takes its maximum at ≈ 240 K. The low-temperature mobility $\mu_{\perp C}(T)$ essentially decreases after the irradiation and varies with temperature according to the law $\mu_{\perp C} \sim \sqrt{1/T}$. Further, the mobility abruptly increases with increasing T and achieves the level of the initial sample.

Although many properties of indium selenide crystals are highly anisotropic, the energy bands forming the fundamental absorption edge are created with significant contribution of p_z-orbitals of Se and have three-dimensional character [20]. Taking into account that for *n*-InSe the effective mass component along the layers is higher than that across to them ($m^*_{\perp C} = 0.31m_0$ and $m^*_{\parallel C} = 0.08m_0$ [21]), in the ideal case of the same scattering mechanism one can expect a low temperature-independent conductivity anisotropy. Just such a situation was observed for *p*-GaSe, a close III–VI group analogue to InSe, where the ratio $\sigma_{\perp C}/\sigma_{\parallel C}$ is ≈ 3.5 at RT that nearly equals to the anisotropy of the corresponding effective masses [22]. But for indium selenide high values of this parameter ($10^2 \div 10^4$) are too far from the effective mass anisotropy. It means that such anisotropy should be considered as defect-induced but not intrinsic.

For impurities in layered InSe crystals their localization in the vdW spaces is energetically more favorable than to be in the ion-covalent layers. That is why dopants, native and residual impurities, first of all interstitial atoms, being affected by high temperature or other factors, can migrate into the interlayer spaces leading to self-purification of the layers. Note that in InSe a majority of impurities including those, which being substitution defects in the layer act as acceptors, between the layers create donor centers [10]. Existing interlayer planar aggregates of donor impurities bend the energy band edges forming potential wells and, therefore, the ranges of two-dimensional electron gas. As a result, the conductivity anisotropy in *n*-InSe increases and appears to be maximum among other layered III–VI crystals. Such thermally stimulated changes in the state of impurities we found earlier for InSe ⟨0.1%Te⟩ crystals annealed in vacuum at 550 °C or only heated to 400 K during measurements. The observed increase of free electron density due to the generation of native In_i donors was related to dissociation of interlayer In inclusions [15]. Another result of such influence is a low value of $\sigma_{\perp C}/\sigma_{\parallel C}$ nearly independent of T. But this state is not equilibrium as after returning to RT the opposite process of impurities' aggregation at the stacking faults takes place. It causes a gradual decrease of n and the formation of the energy barrier, which increases with relaxation time and enhances the anisotropy ratio.

TABLE I

Electrical parameters of n-InSe crystals before and after electron irradiation.

Sample	T[K]	$\sigma_{\perp C}[(\Omega\ \mathrm{cm})^{-1}]$	$n[\mathrm{cm}^{-3}]$	$\mu_{\perp C}[\mathrm{cm}^2/(\mathrm{V\ s})]$	$\sigma_{\parallel C}[(\Omega\ \mathrm{cm})^{-1}]$	$\sigma_{\perp C}/\sigma_{\parallel C}$
1	80	1.67×10^{-2}	1.60×10^{13}	6.51×10^{3}	–	–
	300	7.18×10^{-3}	6.54×10^{13}	6.85×10^{2}	–	–
1E	80	1.65×10^{-3}	2.55×10^{13}	4.04×10^{2}	–	–
	300	6.80×10^{-3}	5.67×10^{13}	7.48×10^{2}	–	–
3[a]	80	4.75×10^{-2}	7.72×10^{13}	3.84×10^{3}	–	–
	300	1.69×10^{-2}	1.49×10^{14}	7.11×10^{2}	–	–
3E[a]	80	9.49×10^{-3}	1.78×10^{14}	3.32×10^{2}	–	–
	300	1.21×10^{-2}	1.56×10^{14}	4.84×10^{2}	–	–
5	80	–	–	–	6.71×10^{-6}	7.08×10^{3}
	300	–	–	–	1.07×10^{-5}	1.59×10^{3}
5E	80	–	–	–	3.79×10^{-8}	2.50×10^{5}
	300	–	–	–	6.01×10^{-6}	2.01×10^{3}
7	80	–	–	–	2.16×10^{-6}	2.20×10^{4}
	300	–	–	–	7.38×10^{-6}	2.29×10^{3}
7E	80	–	–	–	1.35×10^{-8}	7.01×10^{5}
	300	–	–	–	3.81×10^{-6}	3.17×10^{3}

[a]The data for samples 3 and 3E are taken from [17]

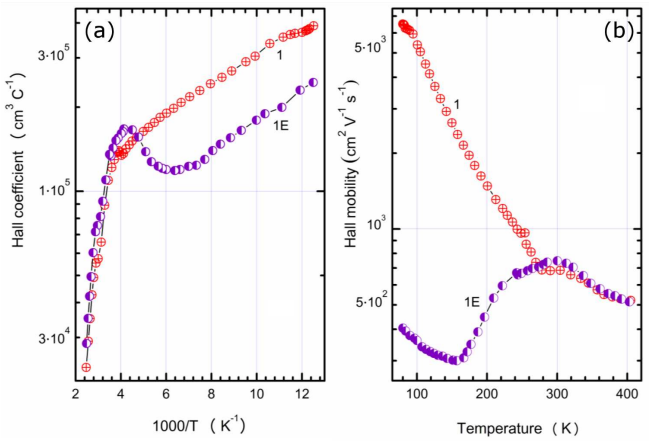

Fig. 3. (a) Typical temperature dependences of the Hall coefficient, and (b) the Hall mobility along the layers for initial sample 1 and e-irradiated sample 1E of n-InSe.

Usually, high-quality InSe crystals grow from a non-stoichiometric melt ($38 \div 48.3\%$ Se). During the growth over-stoichiometric In is rejected to the end of the ingots. However, some amount of the metal remains in the crystals in the form of interstitial atoms that act as shallow donors ($E_d = 18.5$ meV) and determine their n-type conductivity [23]. For instance, the peaks related to In_i atoms were found in the far infrared absorption spectra [13, 24], and the spectra of X-ray photoelectron spectroscopy detected the existence of over-stoichiometric In even in thin exfoliated layers of undoped n-InSe [4]. Therefore, at present it is generally accepted that in undoped InSe crystals just In atoms, accumulated in the vdW gaps, especially at the stacking faults, are mainly responsible for planar aggregates of donor impurities that have decisive influence on conductivity anisotropy. Investigations of InSe⟨Ge⟩ crystals give another piece of evidence of it. For them the optical transitions related to In_i interstitials were not found [24], and electrical characteristics in the range $T < 300$ K are caused not by native In interstitials but by a deeper Ge-related donor. Moreover, on the contrary to a dominant majority of intentionally undoped and doped InSe crystals, we found that annealing in vacuum of Ge-doped samples at temperature as high as 590 °C does not cause the generation the native In_i donors but leads to stabilization of electrical characteristics [25]. As the observed anisotropy ratio in the Ge-doped samples was low and nearly independent of temperature, it was supposed that planar interlayer aggregates of In atoms were absent in these crystals.

Interacting with the InSe lattice high-energy electrons knock out atoms from the sites and create many point defects of donor or acceptor type, e.g., In and Se interstitials and their vacancies. Our previous analysis showed [17] that after e-irradiation with a dose of $10^{14}e$ cm^{-2} the concentrations of donors and acceptors were high and nearly the same, $N_d \approx N_a = (6.9 \div 12) \times 10^{16}$ cm^{-3}. The irradiation also promotes a redistribution of the defects. Therefore their appearance in the layers is followed by segregation into interlayer vdW spaces and accumulation at the stacking faults forming planar aggregates of impurities.

Evidently real InSe crystals contain planar interlayer defects forming potential barriers for transport of charge carriers along the crystallographic C axis. Depending on their width and energy height they determine different mechanisms for charge transfer. To contribute to the conductivity across the layers, carriers should be thermally activated, or tunnel through such barriers.

A distinguished difference between those mechanisms is behaviour of $\sigma_{\parallel C}(T)$ conductivity, which is exponentially dependent or nearly independent of temperature.

Let us suppose that the conductivity across the layers takes place due to thermal activation of free carriers over the energy barrier ΔE_b induced by planar defects. Then in the one-dimensional model for a layered crystal the conductivity $\sigma_{\parallel C}$ can be written as [26]:

$$\sigma_{\parallel C} = en\mu_{\parallel C} \exp\left(-\Delta E_b/k_B T\right). \quad (1)$$

while the conductivity anisotropy can be expressed as

$$\sigma_{\perp C}/\sigma_{\parallel C} = A \exp\left(\Delta E_b/k_B T\right). \quad (2)$$

At the same scattering in n-InSe crystal the pre-exponential factor $A = \mu_{\perp C}/\mu_{\parallel C} = m^*_{\parallel C}/m^*_{\perp C} = 0.615$.

The barrier's value determined for pristine samples 5 and 7 is low and equals to 15.7 and 24 meV, respectively (Table II). It is typical that the values of the pre-exponential factor (746 and 700) are much higher than the effective mass ratio. As it was established [12–14], high conductivity anisotropy in n-InSe was related to the presence of significant concentration of two-dimensional electrons that do not contribute to charge transfer across the layers. Within this model the anisotropy depends on relative value of the densities of 2D and 3D electrons and corresponding mobilities, which is expressed by

$$\frac{\sigma_{\perp C}}{\sigma_{\parallel C}} = \frac{n_2\mu_{2\perp C} + n_3\mu_{3\perp C}}{n_3\mu_{3\parallel C}} \exp\left(\Delta E_b/k_B T\right). \quad (3)$$

Now suppose that the mobility anisotropy for 3D electrons is equal to the effective mass anisotropy $\mu_{3\perp C}/\mu_{3\parallel C} = m^*_{\parallel C}/m^*_{\perp C}$ [14], and the ratio of 3D and 2D electron mobilities along the layers is ≈ 2 [11]. We have determined that $n_2/n_3 \approx 2.41 \times 10^3$ and 2.28×10^3 for initial samples 5 and 7, respectively. This means that two-dimensional carriers are evidently dominant.

The fact that in the pristine InSe samples the $\sigma_{\parallel C}(T)$ conductivity slightly depends on T and is much less than $\sigma_{\perp C}$ can also be explained using model with tunneling carriers through the barrier. The investigated samples were kept long-term before experiments, so it is reasonable to assume that charged interlayer impurities, for instance native In_i donors, could set up high energy barriers for carriers' motion across the layers. In such conditions the expression for anisotropy ratio changes to

$$\frac{\sigma_{\perp C}}{\sigma_{\parallel C}} = \frac{n_2\mu_{2\perp C} + n_3\mu_{3\perp C}}{n_3\mu_{3\parallel C} D}. \quad (4)$$

According to quantum mechanics, the transparence D of a rectangular barrier is

$$D = \frac{16n^2}{(1+n^2)^2} \exp\left(-2d\sqrt{\frac{2m}{\hbar^2}(E_0 - E)}\right), \quad (5)$$

where d is the width of the barrier, E_0 is its height, E is the energy of a particle, m is its mass, and $n = \sqrt{(E_0 - E)/E}$ is the refraction factor.

Since above expression (4) contains many unknown parameters, rigorous calculations are impossible. To estimate the barrier's parameters it was assumed that the energy of a particle is the energy of thermal motion $E = 3k_B T/2$ and also the n_2/n_3 values were used. It is reasonable to suppose that the width of the rectangular tunnel barrier $d = 3$ Å, which in fact is the distance between Se atoms of neighboring InSe layers, is the width of the vacant interlayer gaps. By changing the value of E_0 one can achieve a satisfactory coincidence between the experimental data and calculated dependences (Fig. 2) at the barrier height equal to 0.687 and 1.373 eV for samples 5 and 7, respectively.

TABLE II

Calculated parameters of n-InSe before and after electron irradiation.

Samp.	Charge transfer mechanism along the c axis					
	Activation			Tunelling		
	ΔE_b [meV]	A	n_2/n_3	d [Å]	E_0 [eV]	n_2/n_3
5	15.7	746	2.41×10^3	3.0	0.687	2.41×10^3
5E	32.7	2200	8.22×10^4	–	–	–
7	24.0	700	2.28×10^3	3.0	1.373	2.28×10^3
7E	50.0	710	2.64×10^4	–	–	–

For the pristine InSe samples the available experimental data are insufficient to give advantage to one of the mechanisms above. As for the e-irradiated samples, much higher value and stronger temperature dependence of the anisotropy ratio $\sigma_{\perp C}/\sigma_{\parallel C}$ indicate validity of the activation model. The corresponding calculated curves are shown in Fig. 2, and the numerical data are listed in Table II. For both the samples the e-irradiation resulted in the increase of the energy barrier height by more than twice. Taking into account our data for the mobilities of 2D and 3D electrons along the layers at the same irradiation level [17], as well as supposing that for 3D carriers $\mu_{3\perp C}/\mu_{3\parallel C} = 0.615$ we can more strictly, as compared to the initial samples, determine the concentration n_2/n_3 ratio. The data in Table II (calculations at 80 K) indicate that after the irradiation the relative quantity of 2D electrons also appreciably increases (more than by one order of magnitude).

As a detailed model of 2D electron gas is concerned, the data above are insufficient for its correct choice. However, to explain the obtained results just the existence of 2D electrons is important but not their origination or spectrum of two-dimensional electron states (quantized or continuous). Note that we have not used the model of the 2D subbands at the interface between the γ- and ε-polytypes [11], which predicts space separation of 2D electrons and ionized donors as well as a uniform distribution of shallow donors. In such approach after the e-irradiation these uncompensated donors would provide a significant 3D conductivity in the perfect γ-range which does not agree with our earlier data [17] and the obtained results. That is why we accepted a non-uniform distribution of the shallow donors along the c axis, which additionally becomes stronger after the high-energy e-irradiation.

4. Conclusions

The influence of electron irradiation on conductivity anisotropy in n-InSe is investigated for the first time. The experimental results indicate that the conductivity anisotropy parameter is predominantly affected by planar defects, that promote the formation of potential barriers for charge carriers. They should tunnel through or be activated over them to contribute to conductivity along the c axis. It explains high values $\sigma_{\perp C}/\sigma_{\parallel C}$ for both pristine and irradiated crystals.

Electron irradiation stimulates the transitions of impurities, available in the pristine samples and irradiation-induced ones, into vacant vdW gaps and results in increased anisotropy ratio. The anisotropy, initially high ($\sim 10^4$ at 80 K) but slightly dependent on temperature, abruptly increases after the e-irradiation with a dose of 30 kGy taking extremely high values (nearly 10^6 at 80 K) and varies with temperature according to the exponential law. The results are explained within the model, which along with 3D electrons predicts the presence of 2D carriers not contributing to charge transport along the c axis. The numerical calculations indicate that two-dimensional electrons dominate in all samples and after e-irradiation their relative amount increases by more than a factor of ten, i.e., the significance of 2D electron gas becomes enhanced.

References

[1] G.W. Mudd, S.A. Svatek, T. Ren, et al., *Adv. Mater.* **27**, 714 (2013).

[2] N. Balakrishnan, Z.R. Kudrynskyi, M.W. Fay, et al., *Adv. Opt. Mater.* **2**, 1064 (2014).

[3] G.W. Mudd, S.A. Svatek, L. Hague, et al., *Adv. Mater.* **27**, 3760 (2015).

[4] N. Balakrishnan, Z.R. Kudrynskyi, E.F. Smith, M.W. Fay, O. Makarovsky, Z.D. Kovalyuk, L. Eaves, P.H. Beton, A. Patanè, *2D Mater.* **4**, 025043 (2017).

[5] L.K. Gallos, A.N. Anagnastopoulos, P. Argyrakis, *Phys. Rev. B* **50**, 14643 (1994).

[6] A.N. Anagnostopulos, B. Ploss, *Phys. Status Solidi A* **73**, 91 (1982).

[7] Ph. Houdy, J.L. Maurice, J.M. Besson, J.Y. Laval, A. Chevy, O. Gorochov, *J. Appl. Phys.* **61**, 5267 (1987).

[8] F. Pomer, X. Bonet, A. Segura, A. Chevy, *Phys. Status Solidi B* **145**, 261 (1988).

[9] B. Mari, A. Segura, A. Chevy, *Appl. Phys. A* **46**, 125 (1988).

[10] A. Segura, M.C. Martinez-Tomás, B. Mari, A. Casanovas, *Appl. Phys. A* **44**, 249 (1987).

[11] A. Segura, B. Mari, J. Martinez-Pastor, A. Chevy, *Phys. Rev. B* **43**, 4953 (1991).

[12] J. Riera, A. Segura, A. Chevy, *Appl. Phys. A* **54**, 428 (1992).

[13] J. Martinez-Pastor, A. Segura, A. Chevy, *J. Appl. Phys.* **74**, 3231 (1993).

[14] J. Riera, A. Segura, A. Chevy, *Phys. Status Solidi A* **136**, K47 (1993).

[15] P.I. Savitskii, I.V. Mintyanskii, Z.D. Kovalyuk, *Phys. Status Solidi A* **155**, 451 (1996).

[16] P.I. Savitskii, Z.D. Kovalyuk, I.V. Mintyanskii, *Inorg. Mater.* **32**, 361 (1996).

[17] I.V. Mintyanskii, P.I. Savitskii, Z.D. Kovalyuk, *Phys. Status Solidi B* **252**, 346 (2015).

[18] F. Pomer, J. Navasquillo, *Phys. Status Solidi A* **110**, 585 (1988).

[19] Ph. Schmid, *Nuovo Cim. B* **21**, 258 (1974).

[20] P. Gomes da Costa, R.G. Dandrea, R.F. Wallis, M. Balkanski, *Phys. Rev. B* **48**, 14135 (1993).

[21] E. Kress-Rogers, R.J. Nicholas, J.C. Portal, A. Chevy, *Solid State Commun.* **44**, 379 (1982).

[22] V. Augelli, C. Manfredotti, R. Murri, L. Vasanelli, *Phys. Rev. B* **17**, 3221 (1978).

[23] A. Segura, K. Wünstel, A. Chevy, *Appl. Phys. A* **31**, 139 (1983).

[24] J. Martinez-Pastor, A. Segura, C. Julien, A. Chevy, *Phys. Rev. B* **46**, 4607 (1992).

[25] P.I. Savitskii, Z.D. Kovalyuk, I.V. Mintyanskii, *Bull. Chernivtsi Univ. Phys. Electron.* **79**, 77 (2000).

[26] K. Maschke, H. Overhof, *Phys. Rev. B* **15**, 2058 (1977).